Model predictive control for three-phase split-source inverter-based virtual synchronous generator

Abou-Hussein, Walaa M.; Dabour, Sherif. M.; Hamad, Mostafa S.; Rashad, Essam M.

Model Predictive Control for Three-Phase Split-Source Inverter-Based Virtual Synchronous Generator

Walaa M. Abou-Hussein
Dept. of Mechatronics
Alexandria Higher Institute of
Engineering & Technology
(AIET)
Alexandria, Egypt
walaa.abouhussein@aiet.edu.eg

Sherif. M. Dabour
Dept. of Electrical Power and
Machines Engineering
Tanta University
Tanta, Egypt
shdabour@ieee.org

Mostafa S. Hamad
Dept. of Electrical and Control
Engineering
AASTMT
Alexandria, Egypt
mostafa.hamad@staff.aast.edu

Essam M. Rashad
Dept. of Electrical Power and
Machines Engineering
Tanta University
Tanta, Egypt
emrashad@f-eng.tanta.edu.eg

Abstract—**Realizing local voltage regulation and power-sharing of an islanded AC microgrid can be achieved by conventional control that employs outer-loop droop control and inner-loop cascaded linear control. However, it has limited dynamic response, complex structure, and a rapid rate of change of frequency. In addition, the use of two-stage DC-DC-AC converters for interfacing the renewable energy sources and the microgrid reduces the system efficiency. The split-source inverter (SSI) introduces an alternative single-stage solution for the DC-DC-AC conversion. This paper proposes a virtual synchronous generator (VSG) control algorithm based on model predictive control (MPC) for a three-phase SSI. A finite-set MPC (FS-MPC) is employed to achieve a simple control structure, fast dynamic response, higher stability, and improved current limitation in the inner control loop. A VSG control algorithm without a phase-locked loop is utilized in this paper to achieve active-power-sharing and inertia emulation in the outer control loop. The analysis and modeling of the proposed technique are presented in detail. The simulation results verified the merits of the analysis and the theoretical finding.**

Keywords— Predictive control, split-source inverter, virtual synchronous generator.

I. INTRODUCTION

High penetration of Renewable Energy Sources (RES) leads to various technical challenges such as instability problems of the power system, frequency deviations, and synchronization problems with the grid [1]. These problems are owed to the low-inertia characteristics of nonsynchronous generators' nature, such as the photovoltaic and fuel-cell systems, which are being added to modern power systems with no mechanical kinetic energy [2], [3]. Undoubtedly, the power converters play a critical role in interfacing the RES with the common AC bus of the AC microgrid (MG).

The rotating parts of the synchronous generators and turbines interchange inertial energy with the grid so that the primary controllers have time to react to the grid disturbance or load or generation imbalance. Primary control of voltage source converter (VSCs) comprises two main control loops: an inner loop for local voltage and frequency regulation and an outer loop for power-sharing. In [4], a conventional cascaded dual-loop linear feedback control is employed in the inner loop of the primary control which is suffering from slow dynamic response, high effort for tuning parameters and having a complex structure. Employing droop control for the outer loop doesnot give the required inertia, and hence a high rate of change of inertia occurs in case of disturbances. In [5], [6], current-controlled VSG is introduced in which current control loop is employed. However, it cannot operate in an islanded mode. For islanded mode, a VSG control scheme is presented in [7], [8].

Nevertheless, the control scheme doesnot provide current-limiting capability. In [9]-[11], voltage control and and current control are both applied using cascaded linear control based on VSG scheme. However, this method of control suffers from the same disadvantages given by the conventional linear control.

A fast transient response, optimization with multi-objective ability, simple structure and capability of handling constraints can be provided by model predictive control (MPC) due to its ability to integrate constraints and multiple control objectives into only one cost function (CF). Hence, avoiding the complex structure and the effort in the parameter-tuning process presented by conventional linear control schemes. However, a droop control-based FS-MPC scheme would result in a large rate of change of frequency (RoCoF) [4]. A FS-MPC-based VSG scheme is introduced in [12], considering only fault-ride through capability.

The work in [13] introduces an optimized primary control that combines FS-MPC for the inner loop and voltage-controlled VSG for the outer loop. This achieves a compact structure, faster dynamic response, higher current-limiting capability, robust local voltage, and emulation of inertia for islanded AC microgrids. However, the VSG based on the model predictive control method needs to repeatedly calculate and compare the control targets under different switching states to obtain the optimal switching state, which leads to a long calculation time. Consequently, a control method that can reduce the calculation time of the control system is proposed in [14].

The method proposed in [15] can provide inertia support during transient states and enhance the dynamic characteristics of system voltage and frequency by establishing the prediction model of VSG and designing the cost function for frequency

and power. Hence, the increments of the needed active and reactive power are calculated then superposed on the power reference of VSG. However, an additional DC-DC stage is needed to prevent the boosting limitations presented when using a voltage source inverter (VSI).

DC-AC power converters that gives the buck-boost capability in only one stage are getting high interest. When comparing to the equivalent two-stage converters, they have smaller size, less cost, less weight, and the system is totally less complex [16]–[20]. The most common topology in this power converter category is the conventional Z-source inverter (ZSI) topology introduced in [21]. The ZSI employes four passive elements in addition to a diode carrying the full power to act as a buck-boost stage. However, the ZSI needes another switching state in addition to the conventional eight states and its input current is discontinuous.

A split-source inverter (SSI) topology that utilizes a reduced number of passive elements compared to the ZSI, in addition to a diode for each inverter leg, is proposed in [22]. The three-phase SSI topology integrates the DC/DC boost converter into a three-phase voltage VSI by connecting the boost inductor to the switching nodes of the inverter legs via diodes. Compared with the other counterparts, the SSI has many advantages, like lower component rating, continuous input current, and common DC bus, which led to an investigation of this converter for grid-connected applications, which are now increasingly used in distributed microgrid and smart-grid applications. Moreover, a new cascaded multilevel inverter (MLI) topology is proposed in [23] that extends the idea of the SSI to the cascaded MLI configurations. This topology improves the performance of the conventional single-stage and multilevel boosting topologies to reduce the number of passive elements in each H-bridge unit. Moreover, a split-source nine-switch inverter (NSI) for dual three-phase output operation has been introduced in [24]. This topology reduces the number of active switches by 25% compared to conventional dual output inverters and reduces the number of inductors and capacitors used in the boosting action in the DC-side.

Owing to the previous problems, a MPC-VSG control scheme based on SSI is presented in this paper to optimize conventional primary control for islanded AC MGs and overcome the boosting limitations in grid-connected VSIs.

The rest of this paper is organized in the following way. Section II shows the model of the microgrid. The classical primary control of an AC MG is introduced in Section III. Section IV introduces the proposed scheme of the MPC for split-source inverter-based VSG system. Section V provides the simulation results. Finally, the conclusions of the work are given in Section VI.

II. THE SYSTEM MODEL

An islanded AC microgrid supplied from a three-phase VSC through a LC filter is shown in Fig.1. A dynamic model of the filter is given by (1), where L_f and C_f are the filter inductance and capacitance, respectively.

$$\frac{d}{dt}\begin{bmatrix} i_f \\ v_f \end{bmatrix} = \begin{bmatrix} 0 & -\frac{1}{L_f} \\ \frac{1}{c_f} & 0 \end{bmatrix} \begin{bmatrix} i_f \\ v_f \end{bmatrix} + \begin{bmatrix} \frac{1}{L_f} \\ 0 \end{bmatrix} v_i + \begin{bmatrix} 0 \\ -\frac{1}{c_f} \end{bmatrix} i_o \quad (1)$$

where

$$x = \begin{bmatrix} i_f \\ v_f \end{bmatrix} \qquad\qquad B = \begin{bmatrix} 1/L_f \\ 0 \end{bmatrix}$$

$$A = \begin{bmatrix} 0 & -1/L_f \\ 1/c_f & 0 \end{bmatrix} \qquad B_d = \begin{bmatrix} 0 \\ -1/c_f \end{bmatrix} \quad (2)$$
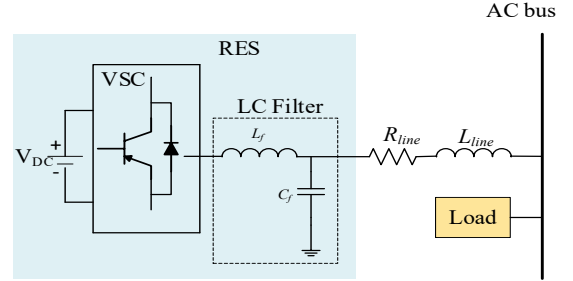

Fig. 1. An AC MG supplied from a three phase VSC through a LC filter in an islanded mode.

The relations of the filter-capacitor voltage v_f, inductor current i_f, inverter output voltage v_i, and load current i_o are defined in the $\alpha - \beta$ frame by (3), (4), (5), and (6) respectively.

$$v_f = v_{f\propto} + v_{f\beta} \quad (3)$$
$$i_f = i_{f\propto} + i_{f\beta} \quad (4)$$
$$v_i = v_{i\propto} + v_{i\beta} \quad (5)$$
$$i_o = i_{o\propto} + i_{o\beta} \quad (6)$$

The total voltage vectors of the inverter output voltage are given in Table I.

III. CONVENTIONAL CONTROL

The conventional control shown in Fig. 2 have a droop control as an outer-loop and a cascaded voltage and current control as an inner-loop.

TABLE I. SWITCHING STATES AND OUTPUT VOLTAGE VECTORS OF THE SSI TOPOLOGY

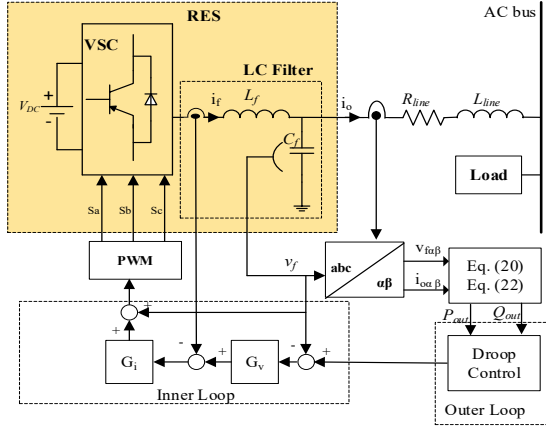| Vector	Switching state $S=[S_1\,S_3\,S_5]$	Output voltage $v_i = [v_{i\alpha}\ v_{i\beta}]$
0	[0 0 0]	[0 0]
1	[1 0 0]	[2V$_{dc}$/3 0]
2	[1 1 0]	[V$_{dc}$/3 √3V$_{dc}$/3]
3	[0 1 0]	[-V$_{dc}$/3 √3V$_{dc}$/3]
4	[0 1 1]	[-2V$_{dc}$/3 0]
5	[0 0 1]	[-V$_{dc}$/3 -√3V$_{dc}$/3]
6	[1 0 1]	[V$_{dc}$/3 -√3V$_{dc}$/3]
7	[1 1 1]	[0 0]

Fig. 2. Block diagram of the conventional control of an AC MG.

A. Droop control

It provides the outer-loop with the reference voltage V_{ref} and reference frequency ω_{ref}. For voltage and frequency stability, the voltage and frequency control must have the characteristics shown in Fig. 3 (a) and Fig. 3 (b), respectively.

$$\omega_{ref} = \omega_n - k_p \left(P_{out} - P_{ref} \right) \qquad (7)$$

$$V_{ref} = V_n - k_q \left(Q_{out} - Q_{ref} \right) \qquad (8)$$

where ω_{ref}, V_{ref}, P_{ref}, ω_n, V_n are reference angular frequency, reference voltage amplitude, reference active power, nominal angular frequency, and nominal voltage amplitude, respectively. K_p and k_q are P-ω and Q-V droop coefficients. P_{out} and Q_{out} are instantaneous active and reactive powers.

B. Cascaded linear control

The inner control loop aims to obtain the desired voltage response for an islanded AC microgrid. A cascaded linear voltage and current is employed where the inner-loop proportional current controller and the outer-loop proportional-resonance voltage controller are defined by

$$G_i(s) = k_{pi} = 2\pi f_{b\omega} L_f \qquad (9)$$

$$G_v(s) = k_{pv} + k_{rv} \frac{s}{s^2 + \omega^2} \qquad (10)$$

where k_{pi} and f_{bw} are the proportional gain and desired bandwidth of the current controller and k_{pv} and k_{rv} are the proportional and resonant gains of the voltage controller.

A new MPC-VSG scheme based on the SSI topology is proposed to avoid the drawbacks of the conventional droop-cascaded linear control and merge the boost and VSI stages in single-stage DC-AC power conversion.

IV. PROPOSED MPC-VSG BASED ON SSI

A model predictive control for a three-phase split source inverter-based virtual synchronous generator is proposed to optimize conventional control for AC microgrids.

A. The three-phase Split-source inverter (SSI)

The three-phase SSI, shown in Fig. 4, uses the same bridge as the conventional three-phase VSI, considering the same eight states. For charging the inductor L_s, the SSI employes at least one of the lower semiconductor switches, S_{al}, S_{bl}, and S_{cl}.

Only one state is used to discharge the inductor and hence charging the inverter DC-link capacitor.

(a) Q-V droop characteristics.   (b) P-ω droop characteristics.
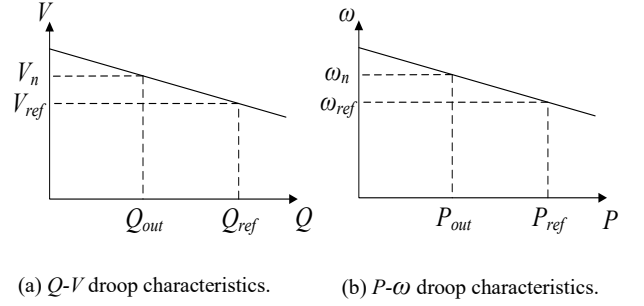
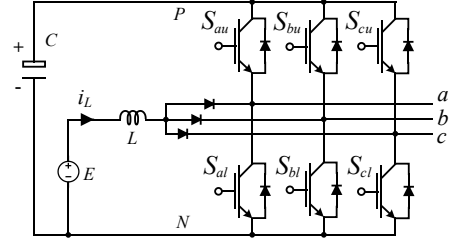Fig. 3. Droop characteristics.

Fig. 4. Three-phase split-source inverter.

The proposed MPC-VSG control block diagram shown in Fig. 5 contains two main parts that are FS-MPC for the inner loop and voltage-controlled VSG for the outer loop. The inner loop aims to reach the required transient response and provide a robust local voltage, while the outer loop is employed to achieve the desired power-sharing and provide a virtual inertia for an islanded AC MG. The converter employed in the proposed scheme is a split-source inverter to avoid using an additional boosting stage required in the conventional VSI due to its step-down limitations.

B. The inner-loop FS-MPC voltage control

Compared to the cascaded linear control, faster dynamic response and higher robustness of the output voltage can be achieved by means of FS-MPC.

According to (1), the discrete-time model for a sampling time T_s is obtained by (11).

$$x(k + 1) = A_q x(k) + B_q v_i(k) + B_{dq} i_o(k) \qquad (11)$$

where

$$A_q = e^{AT_s} \qquad (12)$$

$$B_q = \int_0^{T_s} e^{At} B \, dt \qquad (13)$$

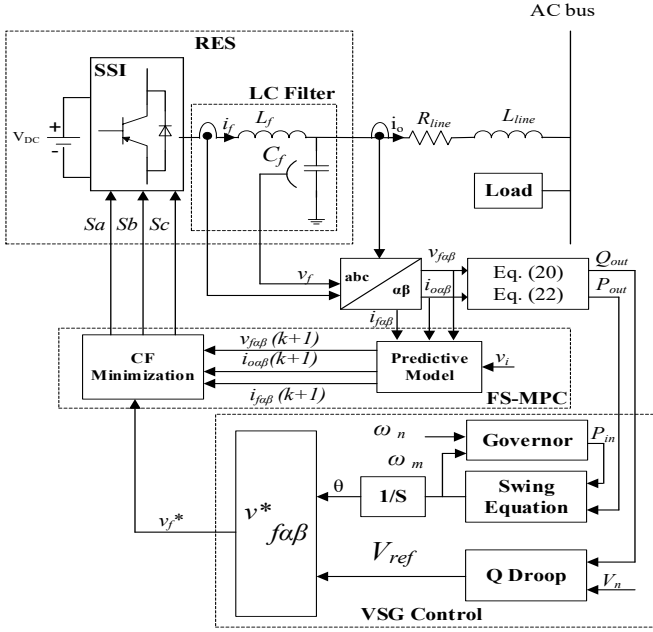$$B_{dq} = \int_0^{T_s} e^{At} B_{dq} \, dt \qquad (14)$$

Fig. 5. Block diagram of the proposed MPC-VSG-based SSI.

FCS-MPC algorithm is shown in Fig. 6. The value of the output voltage $v_f(k)$, the current of the filter's inductor $i_f(k)$ are measured at the instance k. Both the output voltages and the inductor filter current, for every possible voltage vector, at the next instance $v_f(k+1)$ and $i_f(k+1)$ can be predicted using (11). Then, the cost function (15) is employed to choose the voltage vector which minimizes the error between the output voltage and its reference and also the error between the inductor current and its reference at the next instance. Hence, the corresponding switching state is applied in the next instance.

$$g = \left(v_{f\alpha}^* - v_{f\alpha}(k+1)\right)^2 \\ + \left(v_{f\beta}^* - v_{f\beta}(k+1)\right)^2 \\ + \lambda\left(\left(i_{f\alpha}^* - i_{f\alpha}(k+1)\right)^2 \\ + \left(i_{f\beta}^* - i_{f\beta}(k+1)\right)^2\right) \quad (15)$$

where λ is the weighting factor. The reference of the filter-capacitor voltage is

$$v_f^* = V_{ref}cos\left(\omega_{ref}(k)\right) + jV_{ref}sin\left(\omega_{ref}(k)\right) \quad (16)$$

Hence the filter-inductor current can be derived as

$$i_f^* = jC_f\,\omega_{ref}(k)v_f^* + i_o(k) \quad (17)$$

From (17), it could be noticed that the load current is obviously included, and as a result the disturbance in the load current could be integrated. Hence, a robust voltage in case of load disturbance could be easily achieved.

Using FS-MPC, we eliminate the cascaded structure and the modulation delay in the classical linear control with one design parameter λ. Thus we achieve (1) simple control, (2) parameter tuning, and (3) fast dynamic response.
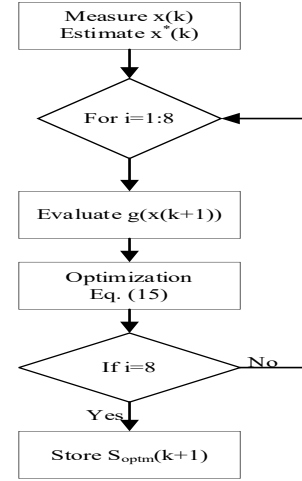

Fig. 6. FCS-MPC algorithm.

C. Voltage-controlled VSG

A voltage-controlled VSG is employed to provide virtual inertia for the AC microgrid. It generates the voltage reference and delivers it to the inner-loop. Fig. 7 shows the three basic parts of the VSG controller, which are governor, swing equation, and reactive power control system.

The function of the governor is to control the active power under deviation in frequency, and it is performed through ω-p droop control

$$P_{in} = P_n - k_\omega(\omega_m - \omega_n) \quad (18)$$

where P_{in} and ω_m are the virtual active power reference and the virtual angular frequency of the VSG, respectively. k_ω is the $\omega - P$ droop coefficient. P_n and ω_n are the nominal active power and the nominal angular frequency, respectively.

The swing equation is employed to emulate the rotor inertia of synchronous generators. It is emulated into the VSG control part as

$$P_{in} - P_{out} - D(\omega_m - \omega_n) = J\omega_n d\left(\frac{\omega_m - \omega_n}{dt}\right) \quad (19)$$

where D, J are damping factors and virtual inertia, respectively. When frequency deviation occurs, J is activated to achieve RoCoF attenuation and hence improving stability of the power frequency.

The active output power of the SSI is given by

$$P_{out} = (v_{f\alpha}i_{o\alpha} - v_{f\beta}i_{o\beta})\frac{\omega_c}{s + \omega_c} \quad (20)$$

The reactive power control is implemented by the Q-V droop control

$$V_{ref} = V_n - k_q(Q_{out} - Q_n) \quad (21)$$

where Q_{out} and Q_n are the reactive power and the nominal reactive power, respectively. The reactive power is given by

$$Q_{out} = (v_{f\beta}i_{o\alpha} - v_{f\alpha}i_{o\beta})\frac{\omega_c}{s + \omega_c} \quad (22)$$

The reference voltage amplitude, V_{ref} and the angular frequency, ω_m will form the reference of the filter voltage v_f^*.
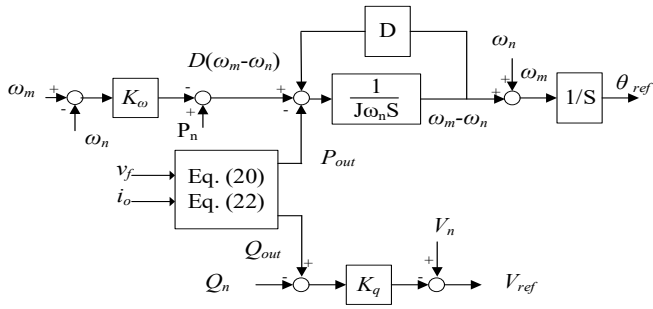

Fig. 7. Block diagram of the voltage-controlled VSG scheme.

V. SIMULATION RESULTS

It is of great importance to show the performance of the proposed MPC-VSG-based SSI shown in Fig. 5. The MPC-VSG-based SSI is simulated using MATLAB /Simulink based on Table II and Table III parameters, where setting P_n and Q_n to 0 kW represents an islanded AC MG autonomously. The weighting factor used in the proposed FS-MPC scheme, is set as $\lambda = 1$.

TABLE II.   SYSTEM PARAMETERS

Description	Value
Nominal voltage, V_n	200V
Nominal frequency, f_n	50Hz
DC bus voltage of VSC, V_{dc}	500V
DC bus voltage of SSI	400V
Output LC filter inductor, L_f	2mH
Output LC filter capacitor, C_f	100μf
Cut-off frequency of low pass filter, ω_c	100Hz
Switching frequency, f_{sw}	8kHz
SSI inductor, L_s	2mH
SSI capacitor, C	3mf

TABLE III.   CONTROLLER PARAMETERS

Symbol	Value
k_ω	$1/2*10^{-3}$
k_q	$5*10^{-3}$
J	0.032kg.m^2
D	0

Fig. 8 shows the response of the system in case of a step change in load using the proposed MPC-VSG. For the presented MPC, less voltage fluctuation can be obtained as shown in Fig. 8 (a). The current response under active load change is given in Fig. 8 (b). Introducing dual objective CF forces the proposed MPC-VSG to operate with comparable steady-state performance as conventional Droop-Linear control. Hence, the proposed method can achieve faster dynamic response, stronger robustness to load disturbances, and desired steady-state performance of local voltage.
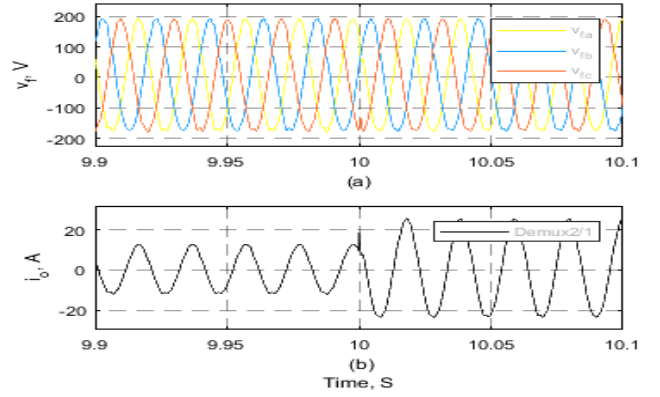

Fig. 8. System response with active load step change. (a) Local voltage response v_f (b) Load current response i_o.

Fig. 9 (a) shows the simulation results of the system frequency response where the frequency changes from 49.8 Hz to 48.6 Hz in 0.09 S under load step change. It can be seen that a small RoCoF is provided by VSG-based control schemes. Hence VSG-based control schemes can increase the system inertia.
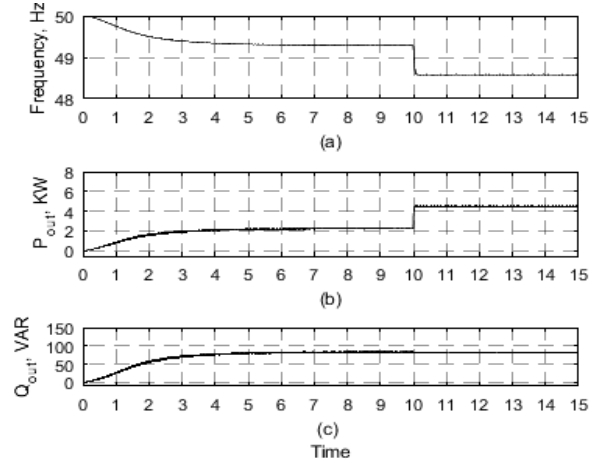

Fig. 9. (a) The system frequency response. (b) The active output power. (c) The reactive output power.

The active power changes from 2.3 kW to 4.6 kW in 0.04 S under active load step change, as shown in Fig. 9 (b). Hence, it can be noticed that by using the proposed technique, a fast transient response can be reached. The reactive output power equals 80 VAR, and it is not affected by the change in the active power, as shown in Fig. 9 (c), which indicates a complete decoupling between the active and reactive power of the system.

Fig. 10 (a) shows that the filter current is tracking its reference value. Considering the SSI used in the proposed MPC-VSG, the DC link capacitor voltage V_{DC} is shown in Fig. 10 (b) and equals 520V from a DC-link voltage of 400V. The boosting inductor current i_{dc} is a continuous current, as shown in Fig. 10 (c). The peak value of the phase voltage at a steady state is 197.2V. Hence, with only one stage, both the boosting stage and the voltage source inverter stage can be achieved in one step with the same standard modulation schemes of the VSI, the same eight switching states of the VSI, and the same number of active switches as the VSI. In addition, a continuous input current can be achieved.

VI. CONCLUSION

A MPC-VSG control scheme for a SSI-based AC microgrid is proposed. The MPC-VSG control is applied to optimize conventional control. First, a split-source inverter is employed to obtain boosting capability without an additional stage and with the same eight switching states of the VSI. Then, a FS-MPC is employed as an inner-loop for the primary control in order to obtain a robust and fast dynamic response of voltage and achieve the capability of limiting the current. Finally, VSG is proposed as an outer-loop to achieve the desired active power-sharing and emulate inertia. The integration of FS-MPC and VSG with SSI achieves enhanced system stability with single-stage boosting inverter operation, proved by simulation results.
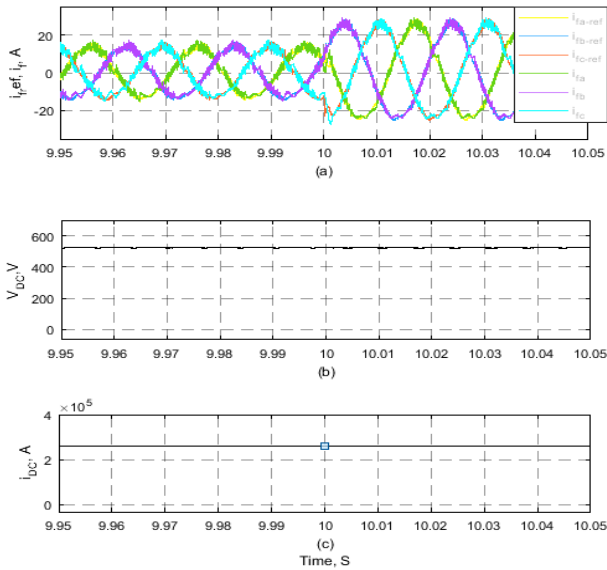

Fig. 10. (a) Filter inductor current i_f and filter inductor current reference i_f^*. (b) The DC capacitor voltage V_{DC}. (c) The boosting inductor current i_{DC}.

The effectiveness of the proposed method considering the transient and steady-state operations for AC MGs is proved by +means of the simulation results.

REFERENCES

[1] J. Zhu, C. D. Booth, G. P. Adam, A. J. Roscoe, and C. G. Bright "Inertia Emulation Control Strategy for VSC-HVDC Transmission Systems," *IEEE Transactions on Power Systems*, vol. 28, no. 2, pp. 1277-1287, May 2013.

[2] A. I. Nkechi, A. M. Howlader and A. Yona "Integration of Photovoltaic Energy to the Grid, Using the Virtual Synchronous Generator Control Technique," *J Energy Power Eng.*, vol. 12, pp. 329-339, 2018.

[3] J. Fang, P. Lin, H. Li, Y. Yang, and Tang, "An Improved Virtual Inertia Control for Three Phase Voltage Source Converters Connected to a Weak Grid," *IEEE Transactions on Power Electronics*, vol. 34, no. 9, pp. 8660-8670, December 2018.

[4] T. Dragicevic, "Model predictive control of power converters for robust and fast operation of ac microgrids," *IEEE Transactions on Power Electronics*, vol. 33, no. 7, pp. 6304–6317, July 2018.

[5] H.-P. Beck and R. Hesse, "Virtual synchronous machine," *2007 9th International Conference on Electrical Power Quality and Utilisation*, October 2007, pp. 1–6.

[6] P. Rodriguez, C. Citro, J. I. Candela, J. Rocabert, and A. Luna, "Flexible grid connection and islanding of SPC-based PV power converters," *IEEE Transactions on Industrial Applications*, vol. 54, no. 3, pp. 2690–2702, May 2018.

[7] J. Liu, Y. Miura, and T. Ise, "Comparison of dynamic characteristics between virtual synchronous generator and droop control in inverter based distributed generators," *IEEE Transactions on Power Electronics*, vol. 31, no. 5, pp. 3600–3611, May 2016.

[8] Q. C. Zhong and G. Weiss, "Synchronverters: inverters that mimic synchronous generators," *IEEE Transactions on Industrial Electronics*, vol. 58, no. 4, pp. 1259–1267, April 2011.

[9] J. Chen, M. Liu, and T. O'Donnell, "Replacement of synchronous generator by virtual synchronous generator in the conventional power system," *2019 IEEE Power & Energy Society General Meeting (PESGM)*, August 2019, pp. 1-5.

[10] X. Meng, J. Liu, and Z. Liu, "A generalized droop control for grid supporting inverter based on comparison between traditional droop control and virtual synchronous generator control," *IEEE Transactions on Power Electronics*, vol. 34, no. 6, pp. 5416–5438, June 2019.

[11] S. D'Arco, J. A. Suul, and O. B. Fosso, "Automatic tuning of cascaded controllers for power converters using eigenvalue parametric sensitivities," *IEEE Transactions on Industrial Applications*, vol. 51, no. 2, pp. 1743–1753, March 2015.

[12] J. Jongudomkarn, J. Liu, and T. Ise, "Virtual synchronous generator control with reliable fault ride-through ability: A solution based on finite set model predictive control," *IEEE Journal of Emerging and Selected Topics in Power Electronics*, vol. 8, no.4, pp. 3811-3824, 2019.

[13] C. Zheng, T. Dragicevi, and F. Blaabjerg, "Model Predictive Control Based Virtual Inertia Emulator for an Islanded AC Microgrid", *IEEE Transactions on Industrial Electronics*, vol. 68, no. 8, pp. 7167-7177, 2020.

[14] Z. Xie, N. Tang, J. Qiu, L. Chen, C. Yuan; "Novel Virtual Synchronous Generator based on Low-Complexity Model Predictive Control", *2021 5th International Conference on Green Energy and Applications (ICGEA)*, 2021, pp. 58-62.

[15] B. Long, Y. Liao, K. T. Chong, J. Rodriguez, J. M. Guerrero, "MPC-Controlled Virtual Synchronous Generator to Enhance Frequency and Voltage Dynamic Performance in Islanded Microgrids", *IEEE Transactions on Smart Grid*, vol.12, no. 2, pp. 953-964, September 2021.

[16] M.-K. Nguyen, Y.-C. Lim, and S.-J. Park, "A comparison between single-phase quasi- z -source and quasi-switched boost inverters," *IEEE Transactions on Industrial Electronics*, vol. 62, no. 10, pp. 6336–6344, October 2015.

[17] J. Cai and Q.-C. Zhong, "An asymmetrical γz-source hybrid power converter with space vector pulse-width modulation," *2014 IEEE Energy Conversion Congress and Exposition (ECCE)*, September 2014, pp. 344–349.

[18] M. Mohr, W. Franke, B. Wittig, and F. Fuchs, "Converter systems for fuel cells in the medium power range;a comparative study," *IEEE Transactions on Industrial Electronics*, vol. 57, no. 6, pp. 2024–2032, June 2010.

[19] A. Hakeem, A. Elserougi, A. El Zawawi, S. Ahmed, and A. Massoud, "A modified capacitor voltage control algorithm for suppressing the effect of measurement noise on grid-connected z-source inverters controllers," *2013 39th Annual Conference of the IEEE Industrial Electronics Society (IECON)*, November 2013, pp. 204–209.

[20] A. Abdelhakim, "Analysis and modulation of the buck-boost voltage source inverter (bbvsi) for lower voltage stresses," *IEEE International Conference on Industrial Technology (ICIT)* , March 2015, pp. 926–934.

[21] F. Z. Peng, "Z-source inverter," *IEEE Transactions on Industrial Applications*, vol. 39, no. 2, pp. 504–510, March 2003.

[22] Ahmed Abdelhakim, Paolo Mattavelli, and Giorgio Spiazzi, "Three-phase Split-Source Inverter (SSI): Analysis and Modulation", *IEEE Transactions on Power Electronics*, vol. 31, no.11, pp. 7451-7461, 2015.

[23] M. AbdulSalam, S. M. Dabour and E. M. Rashad, "Cascaded Multilevel Split-Source Inverters: Analysis and Modulation," *2019 21st International Middle East Power Systems Conference (MEPCON)*, 2019, pp. 1204–1209.

[24] S. M. Dabour, A. S. Abdel-Khalik, S. Ahmed and A. Massoud, "An Optimal PWM Technique for Dual-Output Nine-Switch Boost Inverters With Minimum Passive Component Count," *IEEE Transactions on Power Electronics*, vol. 36, no. 1, pp. 1065–1079, 2021.